Analysis of leaf area index products from combination of MODIS Terra and Aqua data

W. Yang [a,*], N.V. Shabanov [a], D. Huang [a], W. Wang [a], R.E. Dickinson [b], R.R. Nemani [c], Y. Knyazikhin [a], R.B. Myneni [a]

[a] Department of Geography and Environment, Boston University, 675 Commonwealth Avenue, Boston, MA 02215, USA
[b] School of Earth and Atmospheric Sciences, Georgia Institute of Technology, Atlanta, GA 30332, USA
[c] Ecosystem Science and Technology Branch, NASA Ames Research Center, CA 94035, USA

Abstract

A prototype product suite, containing the Terra 8-day, Aqua 8-day, Terra–Aqua combined 8- and 4-day products, was generated as part of testing for the next version (Collection 5) of the MODerate resolution Imaging Spectroradiometer (MODIS) leaf area index (LAI) products. These products were analyzed for consistency between Terra and Aqua retrievals over the following data subsets in North America: single 8-day composite over the whole continent and annual time series over three selected MODIS tiles (1200×1200 km). The potential for combining retrievals from the two sensors to derive improved products by reducing the impact of environmental conditions and temporal compositing period was also explored. The results suggest no significant discrepancies between large area (from continent to MODIS tile) averages of the Terra and Aqua 8-day LAI and surface reflectances products. The differences over smaller regions, however, can be large due to the random nature of residual atmospheric effects. High quality retrievals from the radiative transfer based algorithm can be expected in 90–95% of the pixels with mostly herbaceous cover and about 50–75% of the pixels with woody vegetation during the growing season. The quality of retrievals during the growing season is mostly restricted by aerosol contamination of the MODIS data. The Terra–Aqua combined 8-day product helps to minimize this effect and increases the number of high quality retrievals by 10–20% over woody vegetation. The combined 8-day product does not improve the number of high quality retrievals during the winter period because the extent of snow contamination of Terra and Aqua observations is similar. Likewise, cloud contamination in the single-sensor and combined products is also similar. The LAI magnitudes, seasonal profiles and retrieval quality in the combined 4-day product are comparable to those in the single-sensor 8-day products. Thus, the combined 4-day product doubles the temporal resolution of the seasonal cycle, which facilitates phenology monitoring in application studies during vegetation transition periods. Both Terra and Aqua LAI products show anomalous seasonality in boreal needle leaf forests, due to limitations of the radiative transfer algorithm to model seasonal variations of MODIS surface reflectance data with respect to solar zenith angle. Finally, this study suggests that further improvement of the MODIS LAI products is mainly restricted by the accuracy of the MODIS observations.
© 2006 Elsevier Inc. All rights reserved.

Index terms: MODIS; Terra; Aqua; Leaf area index

1. Introduction

The MODerate resolution Imaging Spectroradiometer (MODIS) on board NASA's Terra and Aqua platforms is designed for monitoring of the Earth's atmosphere, oceans and land surface through operational production of various geophys-

ical products (Justice et al., 2002; Salomonson et al., 1989). Collection 4 represents the latest version of MODIS products and contains the entire time series of data—February 2000 to the present in the case of Terra MODIS and June 2002 to the present in the case of Aqua MODIS. The product suite of both instruments includes vegetation green leaf area index (LAI) and fraction of photosynthetically active radiation (400–700 nm) absorbed by vegetation (FPAR) (Myneni et al., 2002). These products are generated daily at 1 km spatial resolution and composited over an 8-day period. The 8-day products are distributed to the public

* Corresponding author. Fax: +1 617 353 8399.
 E-mail address: ywze@crsa.bu.edu (W. Yang).

from the Land Processes Distributed Active Archive Center (LP DAAC) (WWW1). The Terra MODIS LAI products have been validated with field measurements from a host of vegetation types (Baret et al., 2006; Cohen et al., 2003; Fensholt et al., 2004; Heinsch et al., 2006; Huang et al., 2006; Huemmrich et al., 2005; Morisette et al., 2002, 2006; Privette et al., 2002; Tan et al., 2005a; Wang et al., 2002; Yang et al., 2006a).

The generation of two LAI/FPAR products, one from Terra MODIS and one from Aqua MODIS, that are separated by only 3 h in overpass raises the following questions—(1) how consistent are the two data sets in terms of their spatial-temporal dynamics? and (2) why not combine observations from both instruments to produce a higher quality product? At least the following combined products can be implemented—(1) an improved 8-day product by compositing the 16 daily LAI/FPAR retrievals and (2) a 4-day product by compositing eight daily LAI/FPAR retrievals. The two new products should improve the representation of vegetation in studies on the exchange of fluxes of energy, mass (e.g., water and CO_2), and momentum between the surface and atmosphere (Bonan et al., 2003; Botta et al., 2000; Dickinson et al., 1986; Potter et al., 2003; Tian et al., 2004). In addition, the 4-day product will help to address the following objectives of phenological studies: (a) to monitor the rapid changes (<1 week) in ecosystems during transition periods

of green-up and senescence (Ahl et al., 2006-this issue; Chuine et al., 2000); (b) to monitor the spatial variability of onset of greenness due to variation of the ground temperature and physiology of species (Kang et al., 2003; White et al., 1997; Zhang et al., 2005); (c) to monitor the interannual trends in phenology (4–8 days per two recent decades in advance of spring and delay of fall) (Myneni et al., 1997; Schwartz, 1998; Sparks & Menzel, 2002).

Planning and testing for the next version of MODIS products, Collection 5, is currently under way, with operational processing expected to start in the summer of 2006. We generated a prototype of Collection 5 MODIS LAI/FPAR product suite that includes the following four products—Terra 8-day, Aqua 8-day, Terra–Aqua combined 8- and 4-day. A detailed analysis of the spatial and temporal characteristics of the suite of LAI products is reported in this paper with emphasis on evaluating (1) the consistency between Terra and Aqua products, and (2) the potential for combining retrievals from the two sensors to derive improved products by reducing the impact of environmental conditions and temporal compositing period.

The presentation is organized as follows. The data used in this study and the changes made to the algorithm in Collection 5 are outlined in Section 2. The results are presented and discussed in Section 3 under three broad themes—spatial characteristics,
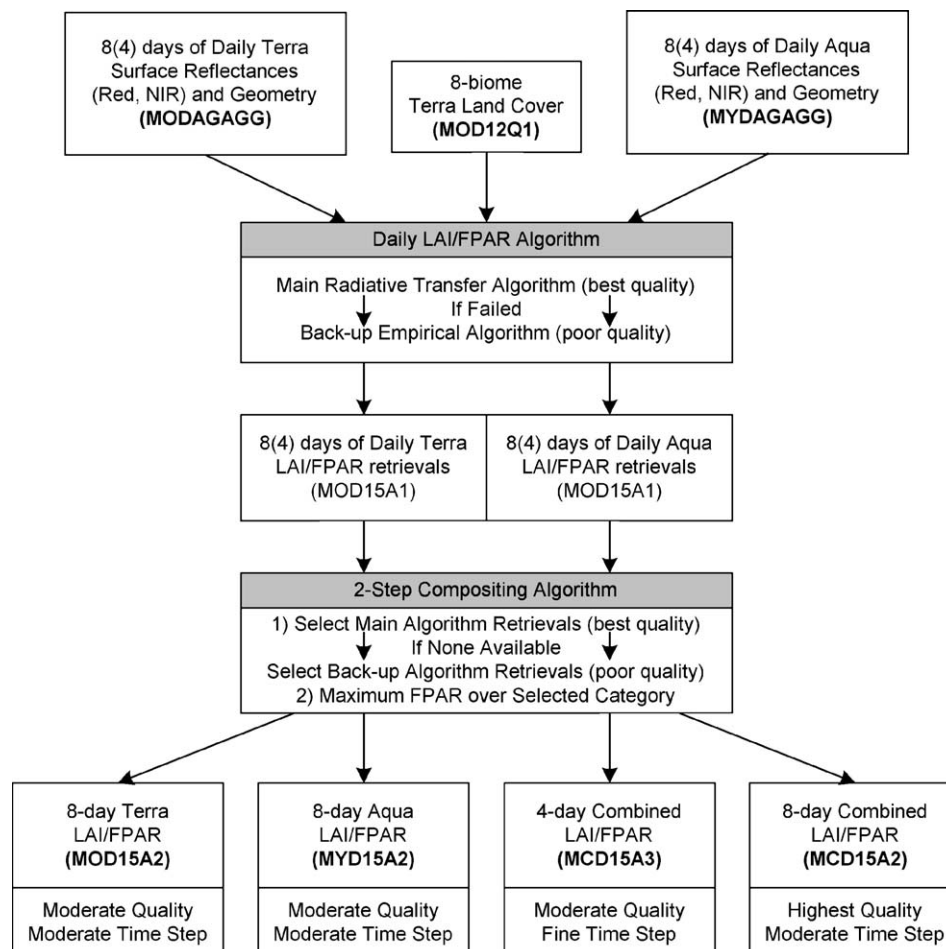

Fig. 1. Production stream of Collection 5 MODIS Terra 8-day, Aqua 8-day, Terra and Aqua combined 8- and 4-day LAI/FPAR products.

seasonal variations and Terra–Aqua LAI anomalies. The paper ends with conclusions in Section 4.

2. Data and algorithms

2.1. Data

The following data products are utilized in this study—(1) Collection 4 atmospherically corrected surface reflectance products from Terra and Aqua MODIS sensors (Vermote et al., 1997, 2002), and (2) Collection 4 land cover product from the Terra MODIS sensor (Friedl et al., 2002). The data are distributed in Sinusoidal gridded format (WWW2), where the Earth surface is divided into 36×18 cells (East–West × North–South), called MODIS tiles ($10° \times 10°$ or 1200×1200 km). Data for 45 MODIS tiles, covering the North American continent during an 8-day composite of Julian days 201–208 (July 20–27) in year 2003, were selected to assess spatial variations, while a time series of data for year 2004 for tiles h12v04 (eastern North America), h11v04 (midwestern USA), and h12v03 (central Canada) were

chosen to analyze temporal variations through the seasonal cycle. Additionally, the following field LAI data (Cohen et al., 2003) and the corresponding 7×7 km MODIS subsets from three sites in North America were utilized in this study: AGRO (broadleaf crops, 40.0066580°N/88.291535°E, MODIS tile h11v04, sample 284, line 1199), NOBS (needle leaf forests, 55.885260°N/98.477268°E, tile h12v03, sample 572, line 493), and HARV (broadleaf forests, 42.528513°N/72.172907°E, tile h12v04, sample 817, line 896).

2.2. Daily LAI retrievals

A schematic plot of operational production of the Collection 5 LAI/FPAR product suite is shown in Fig. 1. The algorithm ingests red and near-infrared surface reflectances, view-illumination geometry, and land cover map to generate daily LAI retrievals for each pixel (Knyazikhin et al., 1998), followed by temporal compositing (details in the next section) to generate a suite of products. The daily LAI retrievals are performed with Look-Up-Table (LUT) approach, where modeled surface
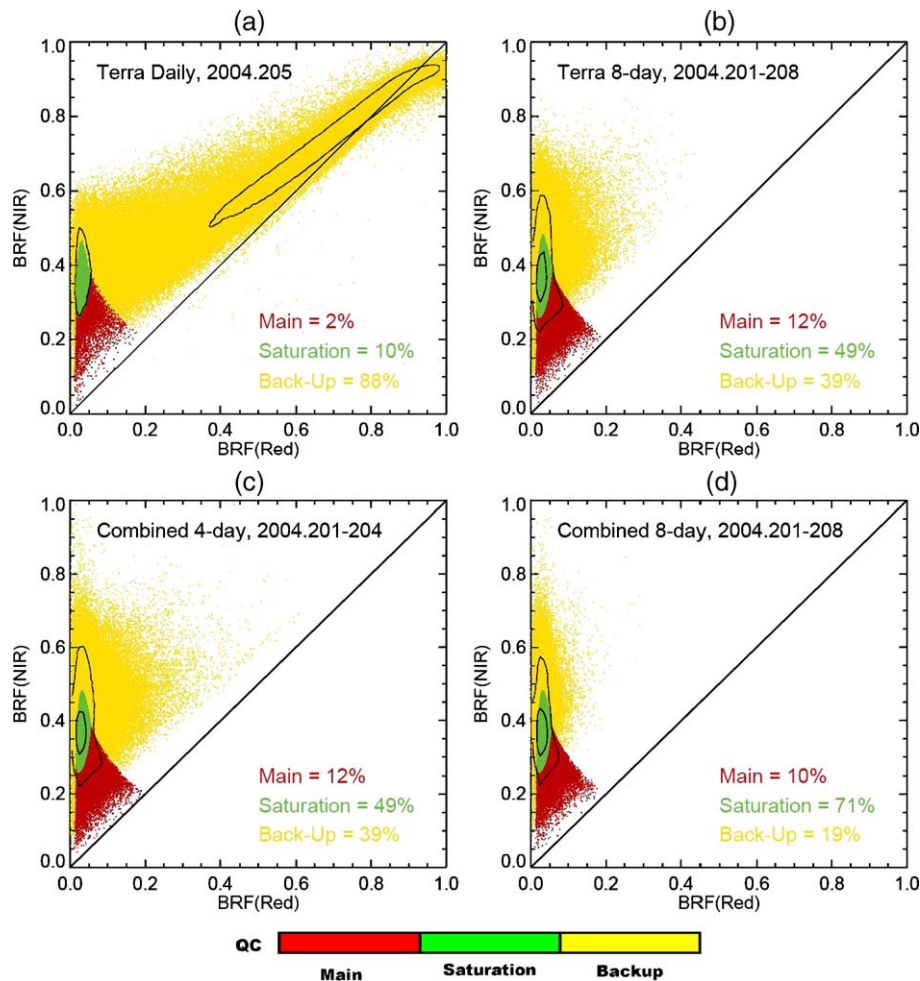

Fig. 2. Impact of compositing on the retrieval domains of main and back-up algorithms in red–NIR spectral space. Retrievals over broadleaf forests pixels in MODIS tile h12v04 are shown. Color coding of MODIS data corresponds to different processing branches of the MODIS LAI/FPAR algorithm—main algorithm without saturation (red), main algorithm with saturation (green), and back-up algorithm (yellow). Contour plots depict 80% (outer contour) and 60% (inner contour) of total density of MODIS data without respect to processing branch. The daily data from Terra MODIS are shown in panel (a), Terra 8-day compositing in panel (b), Terra–Aqua combined 4-day compositing in panel (c), and Terra–Aqua combined 8-day compositing in panel (d).
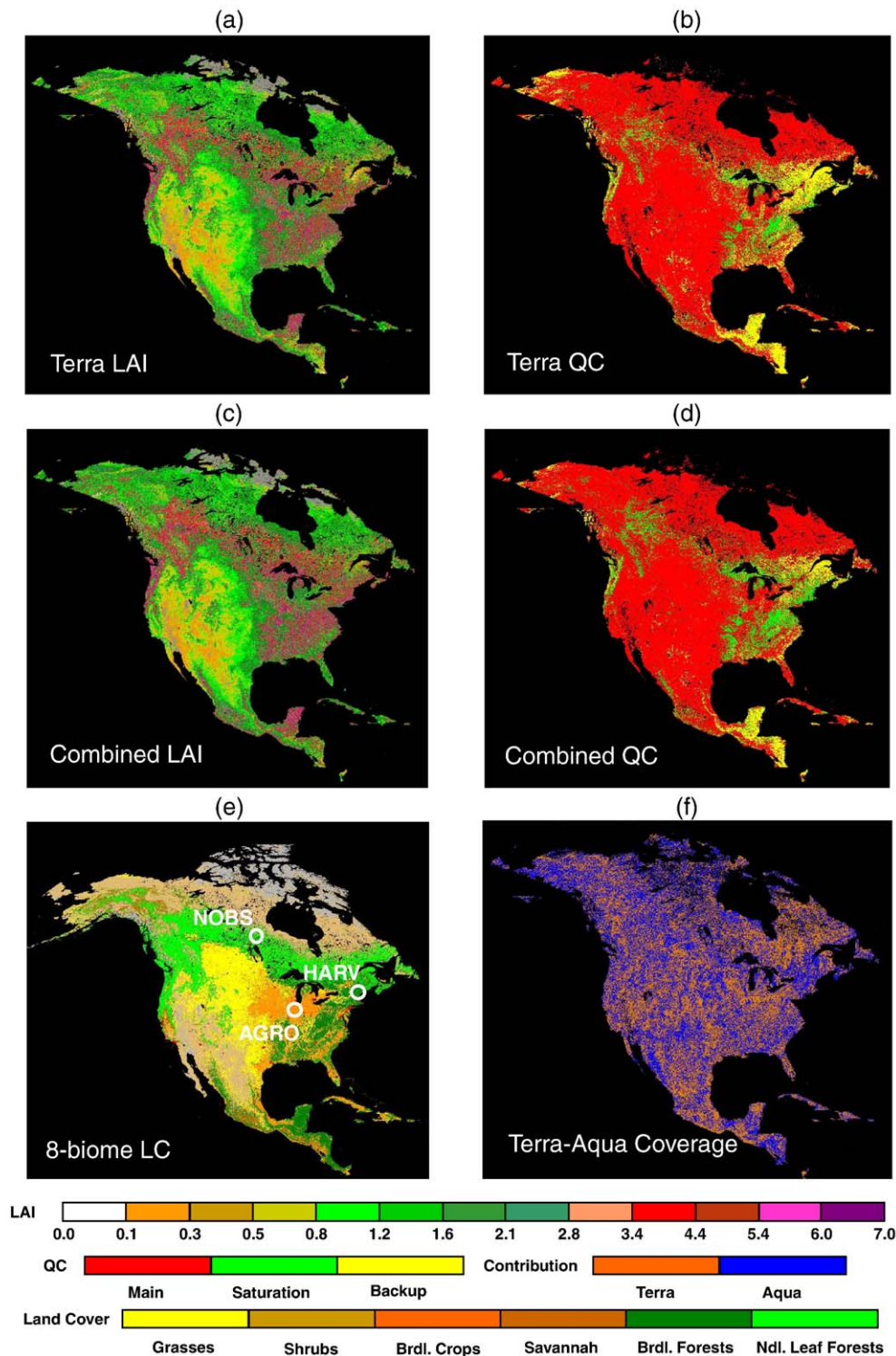
Fig. 3. Comparison of Terra MODIS 8-day and Terra–Aqua combined 8-day retrievals at continental scale (North America) during Julian days 201–208 (July 20–27) in year 2003. The spatial distribution of LAI and QC is shown in panels (a)–(d). The spatial distribution of vegetation types according to the 8-biome Terra MODIS land cover product is shown in panel (e). Circles on land cover map denote location of three validations sites: AGRO (broadleaf crops), NOBS (needle leaf forests), and HARV (broadleaf forests). The spatial distribution of Terra and Aqua MODIS retrievals in combined product ("coverage") is shown in panel (f).

reflectances are parameterized in terms of LAI, vegetation structural, and optical properties, as well as background (soil) optical properties for each land cover type (biome). The Collection 5 algorithm references the 8-biome land cover classification map: (1) grasses and cereal crops, (2) shrubs,

(3) broadleaf crops, (4) savannah, (5) evergreen broadleaf forests, (6) deciduous broadleaf forests, (7) evergreen needle leaf forests, (8) deciduous needle leaf forests.

The retrievals are stored as LAI and corresponding quality control (QC) data layers in the product. The key indicator of the

Table 1
Comparison of Terra MODIS 8-day and Terra–Aqua combined 8-day (in parentheses) retrievals as function of biome type over North America during Julian days 201–208 (July 20–27) in year 2003

	Grasses and cereal crops	Shrubs	Broadleaf crops	Savannah	Broadleaf forests	Needle leaf forests
Land cover						
LC, %	17	27	8	9	14	25
Surface reflectances						
Red	0.049 (0.047)	0.045 (0.045)	0.035 (0.035)	0.034 (0.034)	0.025 (0.025)	0.024 (0.025)
NIR	0.296 (0.304)	0.282 (0.279)	0.381 (0.381)	0.236 (0.238)	0.338 (0.340)	0.219 (0.221)
Leaf area index						
LAI	1.5 (1.7)	1.1 (1.2)	2.0 (2.0)	1.5 (1.6)	4.3 (4.6)	2.7 (3.0)
Quality control						
Main, %	89 (90)	94 (97)	88 (94)	91 (96)	11 (11)	69 (70)
Saturation, %	4 (7)	<1 (<1)	2 (3)	<1 (<1)	32 (44)	11 (18)
Back-up, %	7 (3)	6 (3)	10 (4)	8 (4)	58 (45)	20 (12)
Contribution						
Terra/Aqua, %	53:47	53:47	57:43	53:47	50:50	57:43
Environmental effects						
Clouds, %	15 (17)	13 (12)	17 (15)	18 (16)	32 (25)	11 (8)
Aerosols, %	60 (64)	59 (61)	63 (65)	59 (63)	46 (52)	51 (54)

quality of retrievals is the algorithm path, which distinguishes the following three categories. Best quality, high precision retrievals are obtained from the main radiative transfer (RT) based algorithm in case of low LAI (<3). If LAI is high, surface reflectances have low sensitivity to LAI and the main algorithm retrievals are obtained under reflectance saturation conditions (moderate precision). In the case of main algorithm failure, low precision retrievals are obtained from the back-up algorithm that is based on NDVI–LAI relationships. The algorithm path is therefore a key quality indicator and is stored in the quality control (QC) layer of the MODIS LAI/FPAR products. In addition to algorithm path, the QC layer provides information about presence of clouds, aerosols, and snow, inherited from input surface reflectances products.

For Collection 5 production, substantial modifications to the LUTs of the main algorithm were implemented to improve retrieval quality. Earlier versions of the MODIS LAI products exhibited LAI overestimation and too few main algorithm retrievals in some areas during the growing season. These anomalies over herbaceous vegetation were resolved in Collection 4 (Tan et al., 2005b). In Collection 5, the LUTs for all biomes were recalculated based on the stochastic radiative transfer model (Shabanov et al., 2000, 2005), the parameters of which were selected to model a majority of MODIS surface reflectances. A major focus of Collection 5 refinements was on woody vegetation—broadleaf and needle leaf forests classes were subdivided into deciduous and evergreen subclasses and separate LUTs were developed for each subclass (Shabanov et al., 2005). Additionally, biome-dependent uncertainties, that is, threshold on allowable discrepancies between simulated and MODIS surface reflectances were introduced in Collection 5: 20% at red and 5% at NIR for herbaceous vegetation, 30% at red and 15% at NIR for woody vegetation.

2.3. Temporal compositing

A common temporal compositing approach is used to generate Terra 8-day, Aqua 8-day, Terra–Aqua combined 8- and 4-day products from daily Terra and Aqua retrievals. The compositing periods are non-overlapping. The compositing algorithm is a two-step scheme (Fig. 1)—(1) the retrievals are selected according to algorithm path: main algorithm retrievals have the highest priority, if none available, back-up algorithm retrievals are selected; (2) the LAI value is selected based on maximum FPAR value from the above subgroup of retrievals. The impact of compositing on retrieval domain is shown in Fig. 2 where the red and near-infrared reflectances corresponding to different algorithm paths are plotted. Compositing is effective in removing contaminated retrievals (aerosols, clouds, cf. King et al., 1992)—compare for instance daily retrievals and Terra 8-day composited retrievals (Fig. 2a–b). The back-up algorithm retrievals remaining in Terra 8-day composite are due to residual contamination of surface reflectances or limitations of RT modeling (restrictions on variability of leaf optical properties, soil patterns, canopy structural parameters, etc.). The former effect can be minimized if more observations are available—compare for instance retrievals from 8 observations (Fig. 2b–c) and 16 observations (Fig. 2d). Thus, compositing reduces the impact of day-to-day variations in surface reflectances that are due to cloud and residual atmospheric effects.

3. Results and discussion

3.1. Spatial characteristics

The spatial distribution of LAI over North America shown in Fig. 3 which is an 8-day composite of Julian days 201–208 (July 20–27) in year 2003 shows no visibly distinguishable difference between single-sensor and combined products either in the pattern or the magnitude. Namely, more than 88% of all land vegetated pixels have difference less than 0.5 LAI units, and pixels with larger difference are distributed randomly over forested regions. The LAI spatial patterns closely follow the land cover distribution (Fig. 3e)—high LAI over woody vegetation (especially over broadleaf forests) and low LAI over herbaceous vegetation (especially over shrublands).
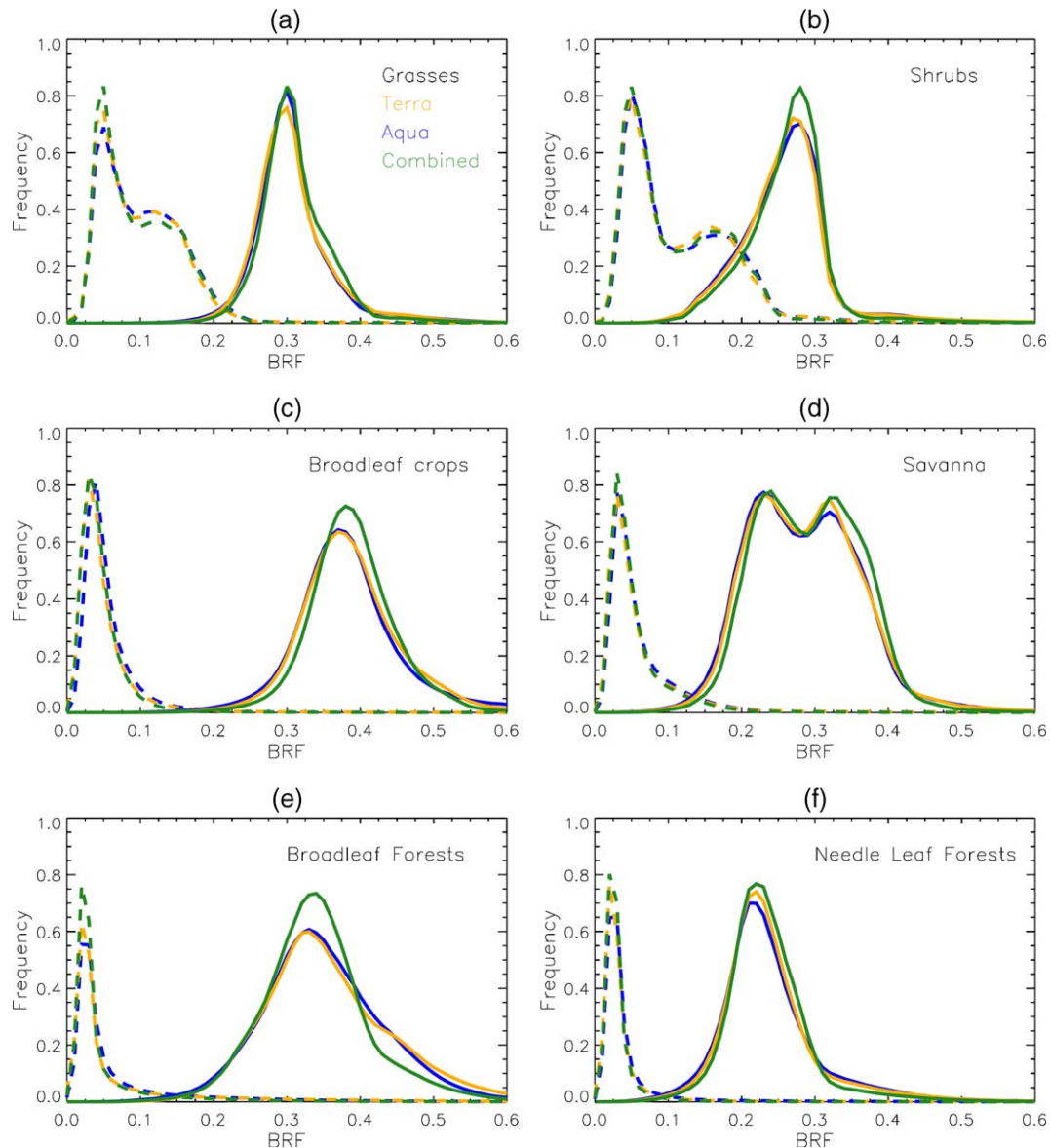
Fig. 4. Comparison of Terra MODIS 8-day, Aqua MODIS 8-day, and Terra–Aqua combined 8-day surface reflectances at continental scale (North America) during Julian days 201–208 (July 20–27) in year 2003. Histograms of red reflectances are shown by dashed lines and near-infrared reflectances with solid lines, for different land cover types.

Overall, the main algorithm retrievals constitute 90–95% of retrievals over herbaceous vegetation and 50–75% over woody vegetation (Table 1). This difference in main algorithm retrieval rate is due to features of the retrieval domain in the red/near-infrared spectral space (cf. Fig. 2). This domain is large for canopies with low LAI values (herbaceous vegetation) and thus retrievals have moderate sensitivity to uncertainties in surface reflectances. The retrieval domain is a compact region in the spectral space (low red and high near-infrared reflectances) for dense, high LAI canopies (woody vegetation)—surface reflectances may fall outside of this region even if they are minimally contaminated with atmospheric effects, in which case the main algorithm fails and the back-up algorithm is triggered (cf. Fig. 2). When the number of observations is increased from eight (as in Terra 8-day product) to 16 (as in combined 8-day product), the retrieval rate of the main algorithm is increased by 10–20%

(Table 1). Finally, note that Terra and Aqua observations contribute about equally to the combined product retrievals for all biome types (Table 1) and the spatial pattern of Terra and Aqua based retrievals is apparently random (Fig. 3f).

The general consistency between Terra and Aqua LAI products seen in Fig. 3 can be understood by analyzing the surface reflectances from the two instruments. While local observation geometry and atmospheric conditions may be different for Terra and Aqua MODIS observations, the continental scale averages of surface reflectances, and thus LAI, show excellent consistency between the two sensors (Figs. 4 and 5 and Table 1). The histograms of red and near-infrared reflectances exhibit substantial differences across vegetation types, such as the bi-modal distributions for savannas, grasses, and shrubs, and generally lower red reflectance values for woody vegetation compared to herbaceous vegetation (Fig. 4). The sharp variations in LAI
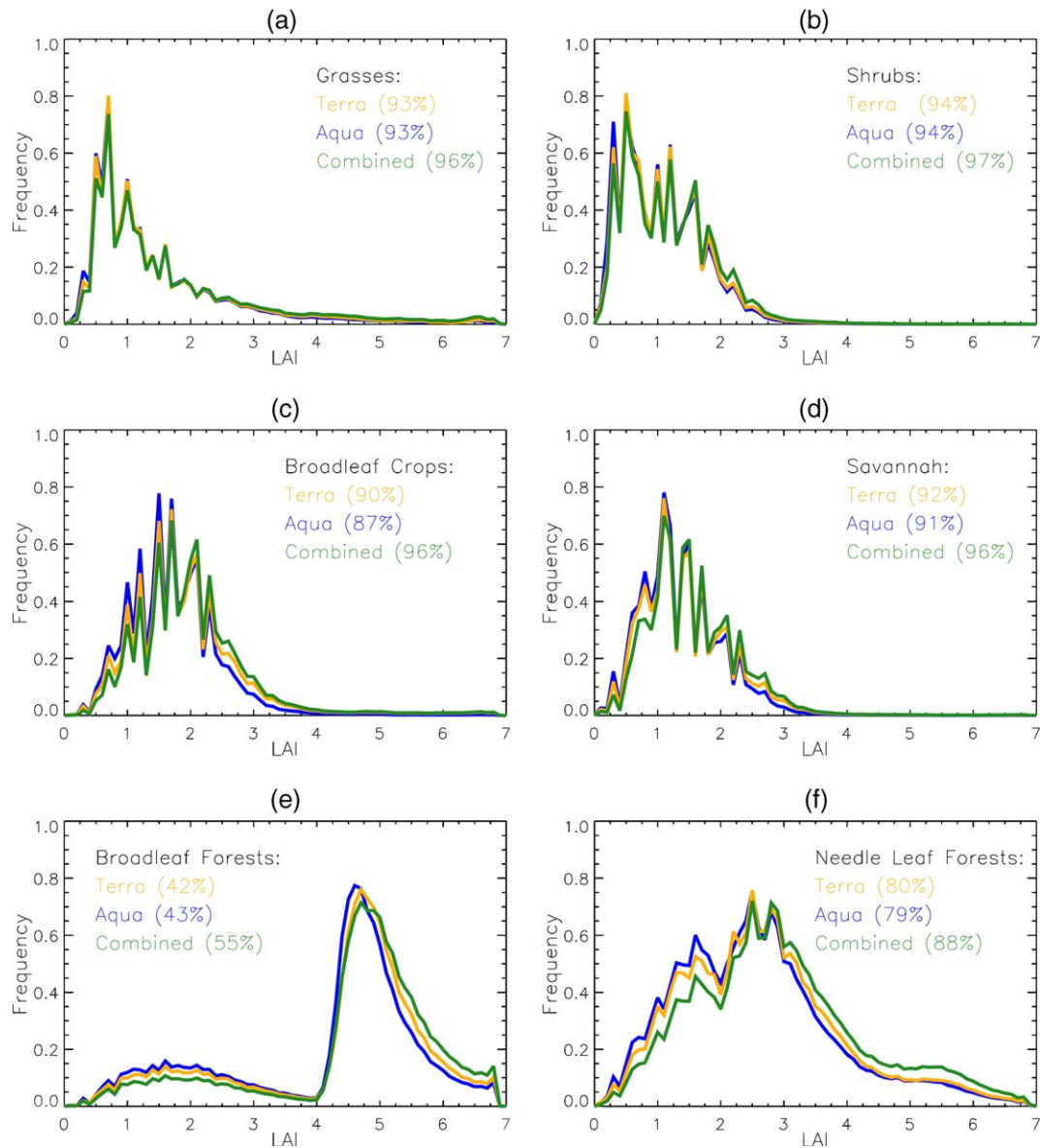
Fig. 5. Comparison of Terra MODIS 8-day, Aqua MODIS 8-day, and Terra–Aqua combined 8-day LAI retrievals at continental scale (North America) during Julian days 201–208 (July 20–27) in year 2003. Histograms of LAI retrieved by main algorithm (with or without saturation) are shown as function of land cover type. Percentages in each panel indicate proportion of main algorithm retrievals in total retrievals.

histograms (Fig. 5) at low LAI values is due to the statistical nature of LAI retrievals—the algorithm reports a single solution, in 0.1 LAI intervals, at low LAI values. Multiple solutions are acceptable at high LAI values, due to low reflectance sensitivity to LAI, and as these solutions are averaged, the histograms tend to be smoother at high LAI values.

3.2. Seasonal variations

Seasonal variations in Terra 8-day, Aqua 8-day, and combined 8- and 4-day retrievals during year 2004 are shown in Figs. 6–10. The analysis was focused on broadleaf crops in tile h11v04 (midwestern USA), broadleaf forests in tile h12v04 (eastern North America), and needle leaf forests in tile h12v03 (central Canada), which contain the three validation sites mentioned in Section 2.1.

The retrievals over broadleaf crops (Fig. 6a–b) demonstrate expected seasonality in LAI with a seasonal maximum LAI between 2 and 3. The LAI from all three products is consistent to within specifications (0.5 LAI). About 80–90% of the retrievals are from the main algorithm without saturation, with the exception of a few winter season composites. The combined product further improves the main algorithm retrievals by 5–10% during the growing season. The retrievals over broadleaf forests (Fig. 6c–d) show LAI values of about 1 during winter and about 4.5 during the growing season. Between 70% and 90% of the retrievals are from the main algorithm during the growing season, but most of these are obtained under conditions of reflectance saturation due to high LAI values of these canopies. The combined product helps to increase main algorithm retrievals in the product by about 15–20%.
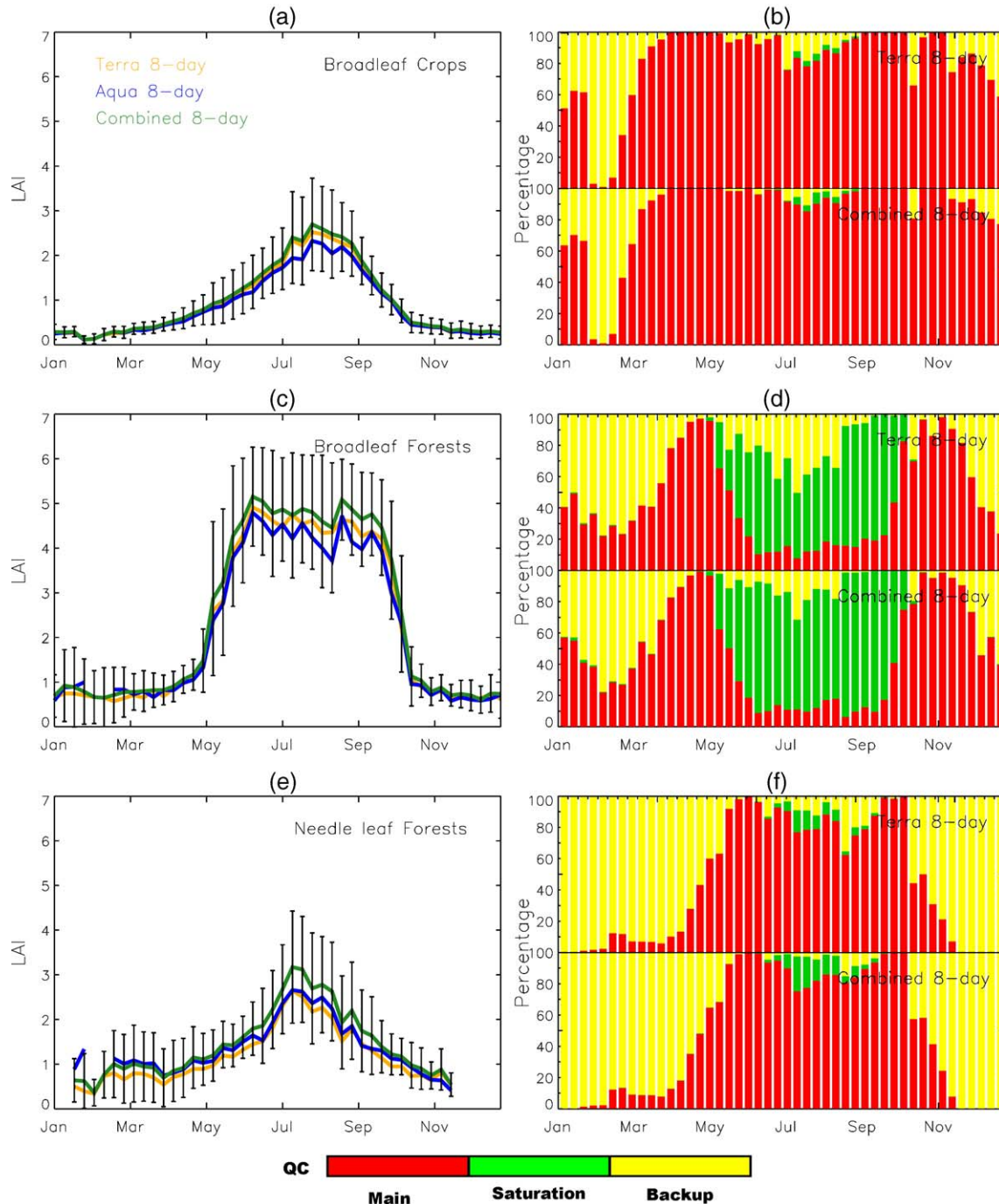
Fig. 6. Comparison of seasonal variations in Terra MODIS 8-day, Aqua MODIS 8-day, and Terra–Aqua combined 8-day LAI retrievals at the scale of a MODIS tile, for three different vegetation types. Panels (a) and (b) show seasonal variations in mean LAI retrieved by the main algorithm (with and without saturation) and QC for broadleaf crops in MODIS tile h11v04. Panels (c) and (d) show the same but for broadleaf forests in tile h12v04. Panels (e) and (f) present results for needle leaf forests in tile h12v03.

The seasonal variations in LAI and QC of needle leaf forests, shown in Fig. 6e–f, exhibit changes in LAI from about 1 in winter to 3 in summer. The QC annual cycle indicates mostly main algorithm retrievals (about 90%) during the growing season. The few main algorithm retrievals in the winter time are due to snow, cloud cover, and high solar zenith angles. The combined product helps to increase the main algorithm retrievals in the product by 5–10% during the growing season, but not for

winter. These results indicate significant LAI seasonality, which can also be seen in other MODIS products, such as NDVI and EVI (WWW3; WWW4)—this is further analyzed in the next section.

The annual course of combined 4-day LAI product resembles those of the single sensor 8-day products in all three biomes (Fig. 7a,c,e). The combined 4-day product QC shows slightly higher composite-to-composite variability. Decreasing the
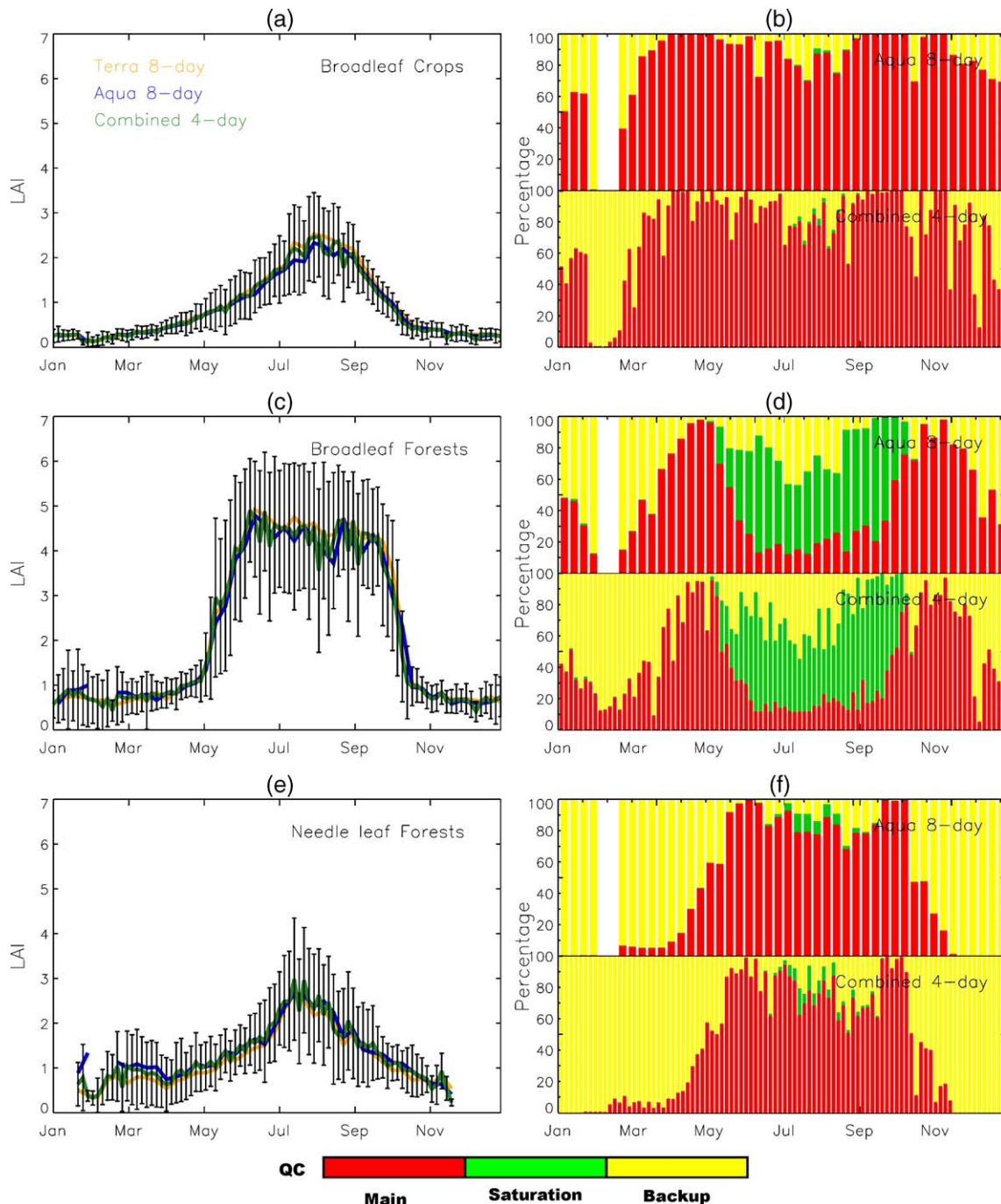
Fig. 7. Same as Fig. 6, except LAI profile is for Terra–Aqua combined 4-day (not combined 8-day) product and QC profile is for Aqua 8-day (not Terra 8-day) and combined 4-day (not combined 8-day) products.

compositing period, from 8 to 4 days, does not greatly decrease the number of main algorithm retrievals included in the product. This is because environmental conditions (such as clouds), which impact algorithm path, are only weakly correlated in the 3-h time shift between Terra and Aqua overpaths. Therefore, for compositing purposes, Terra and Aqua MODIS observations acquired in 3 h or 1-day apart may be treated as bearing equivalent information content.

The extent of cloud and aerosol contamination in Terra 8-day, combined 8- and 4-day LAI retrievals is investigated next

(Fig. 8). Analysis of cloud contamination was performed by referencing MODIS surface reflectance quality control data which identifies four categories of cloud contamination: "cloud state not defined, assumed clear", "clear", "partially cloudy", and "cloudy". We joined the first two and last two categories to derive a "no-cloud and cloud" mask. Similarly, the quality control information about aerosols contained in the MODIS surface reflectance product ("no or low atmospheric aerosols levels detected" and "average or high aerosols levels detected") was used to define "no aerosols and aerosols" mask. Finally, this
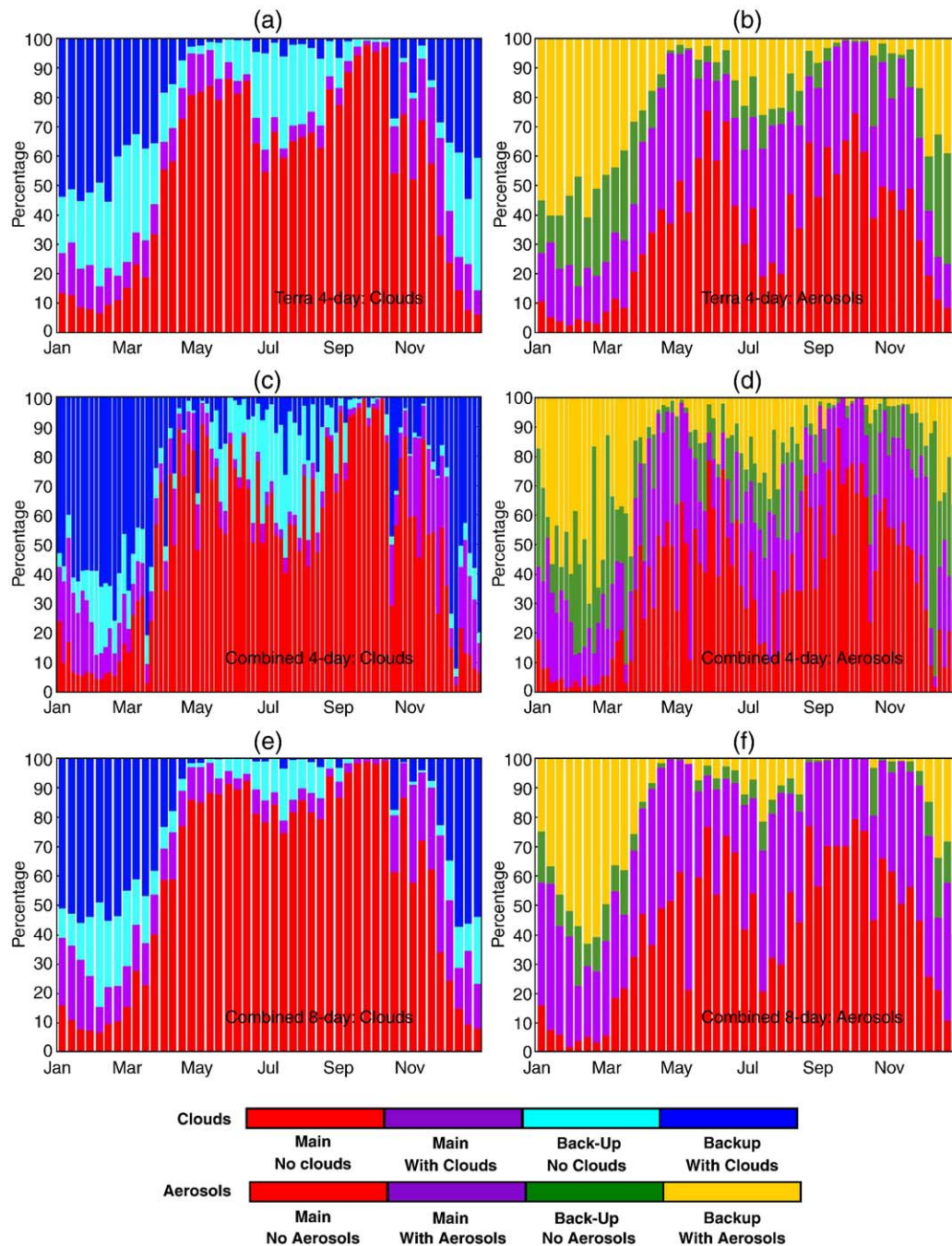
Fig. 8. Impact of cloud (left panels) and aerosol (right panels) contamination on algorithm path. Retrievals from broadleaf forests in MODIS tile h12v04 are shown. Panels (a) and (b) show results for Terra MODIS 8-day product, panels (c) and (d) for Terra–Aqua combined 4-day product, and panels (e) and (f) for Terra–Aqua combined 8-day product.

analysis was restricted to broadleaf forest pixels in tile h12v04 (eastern North America).

In the case of clouds, the retrievals were separated into four categories—main or back-up algorithm path and with or without cloud. Similarly, four categories were defined for aerosols. Retrievals during the growing season are minimally contaminated by clouds: Terra 8-day and combined 8-day products have <10% cloud contaminated retrievals; combined 4-day product has about 15% cloud contaminated retrievals. Cloud contamination can reach up to 70% during winter, spring, and fall seasons. Retrievals under

cloudy conditions are mostly performed by the back-up algorithm as the main algorithm fails as expected (Yang et al., 2006b).

Surface reflectances, and therefore LAI retrievals, under conditions of frequent aerosol contamination are seen during winter (with a maximum in February) and a secondary peak in summer (with a maximum in July). Conditions of minimum aerosol contamination are seen during spring (May–June) and fall (September–October). The seasonality of aerosol properties was explored with sunphotometers ground measurements, initially, over few sites in the US (Flowers et al., 1969; Peterson

(a)

Terra: y=1.02*x+1.21, R^2=0.58
Combined: y=-0.93*x+1.26, R^2=0.65

(b)

Aerosols

- Main, Terra 8-day
- Back-Up, Terra 8-day
- Main, Combined 8-day
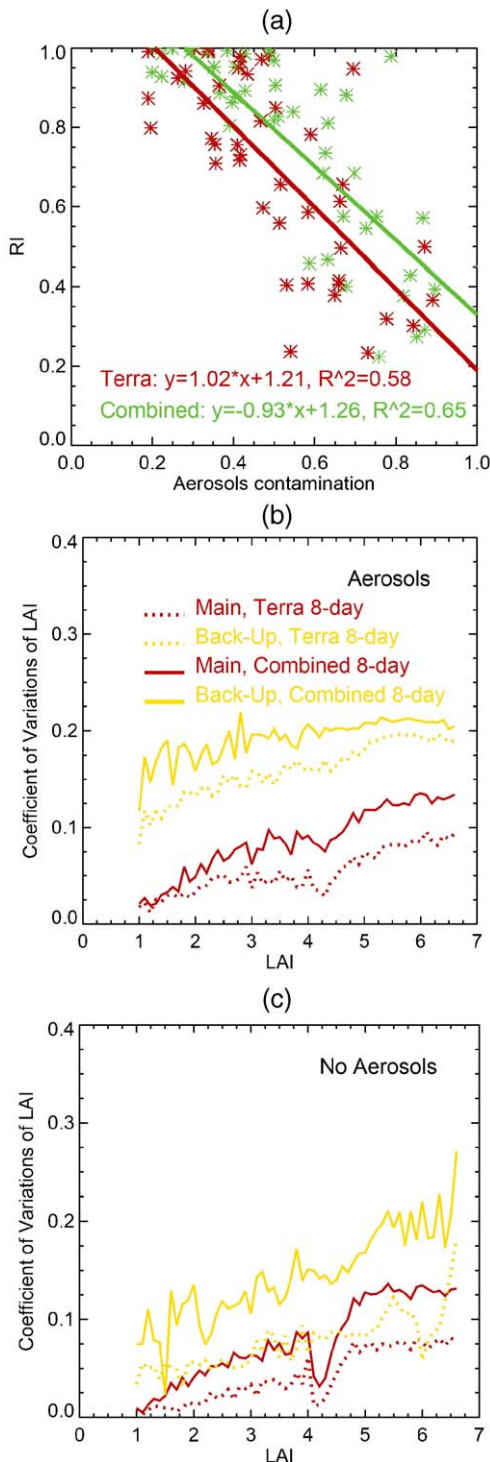- Back-Up, Combined 8-day

(c)

No Aerosols

Fig. 9. Impact of aerosols on quality of Terra and combined 8-day LAI products. Panel (a) shows regression of Retrieval Index (RI) with respect to aerosol contamination. Data are for composites during the growing season, May to October in year 2004, broadleaf forests pixels in tile h12v04. Panels (b) and (c) compare variations in daily LAI, retrieved by main and back-up algorithms with and without aerosol contamination, respectively. Data are for composite for Julian days 201–208 (July 20–27) in year 2004, broadleaf forests pixels in tile h12v04.

et al., 1981) and, later, over global network of AERONET sites (WWW5; Holben et al., 2001). Significant variability of aerosol regimes was observed over the globe: tropical biomass burning, boreal forest, midlatitude dry or humid climates, desert, oceanic

sites, etc. (Kobayashi & Dye, 2005; Ramanathan et al., 2001). Ground measurements over Eastern North America indicate distinct seasonality in aerosol optical depth with maximum both in mean and standard deviation during summer. This phenomenon was attributed to a dynamic mixture of natural and antropogenic sources, processed by convection within humid and hot air masses (Holben et al., 2001).

Fig. 9 provides additional details on aerosol impacts on the quality of LAI retrievals. For each composite during the growing season, May to October in year 2004, broadleaf forests pixels in tile h12v04, two quantities were evaluated: ratio of pixels with retrievals under aerosols to total amount of retrievals (called "aerosol contamination"), and ratio of pixels with retrievals by main algorithm to total retrievals (called "retrievals index", or RI). The regression of aerosol contamination on RI is shown in Fig. 9a. These results indicate rapid decrease in RI as aerosol contamination increases and the correlation is fairly strong: $r^2 = 0.58$ for Terra 8-day and $r^2 = 0.65$ for the combined 8-day products.

Next, consider Fig. 9b–c, which show variability in retrieved LAI (coefficient of variation=standard deviations/mean) during the 8-day composting period as a function of LAI values for two cases: retrievals with and without aerosols contamination. The analysis was performed for composite for Julian days 201–208 (July 20–27) in year 2004, broadleaf forests pixels in tile h12v04. Aerosols generally increase variations in retrieved LAI, as expressed through coefficient of variations, compared to no-aerosol case. The back-up algorithm retrievals have higher variations compared to main algorithm retrievals. Thus, while the combined product does not decrease the total number of retrievals under aerosol contamination, it does increase number of main algorithm retrievals, which results in a higher precision product.

Next, we analyzed the time series of Terra 8-day, Aqua 8-day, and combined 8-day retrievals over a 7×7 km area at three FLUXNET validation sites: AGRO (broadleaf crops), NOBS (needle leaf forests), and HARV (broadleaf forests) (cf. Section 2.1). The location of these sites is shown in Fig. 3e. The annual course of LAI generated by the main algorithm, with or without saturation, at the three sites is shown in Fig. 10. The LAI products agree with field measurements of Cohen et al. (2003), to within uncertainties of both data sets. These small area average LAI values exhibit considerably more variability than the large area averages shown earlier (Figs. 6 and 7), which is to be expected given the areal extent of averaging. Note also that the combined 8-day product tends to decrease random variations in retrievals, if at least one sensor provides accurate estimates of LAI. The reasons for anomalous variations in retrieved LAI are analyzed in the next section.

3.3. LAI anomalies

We selected two composites, Julian days 161–168 (June 9–16) and 225–232 (August 12–19) in year 2004, to investigate a discrepancy in HARV forest LAI values between Terra MODIS (about 5) and Aqua MODIS (about 2–3) (cf. Fig. 10c). A scatter plot of Terra MODIS surface reflectances of all broadleaf forests pixels in tile h12v04 is shown in Fig. 11a–b. The two panels also show Terra and Aqua surface reflectances from the HARV forest
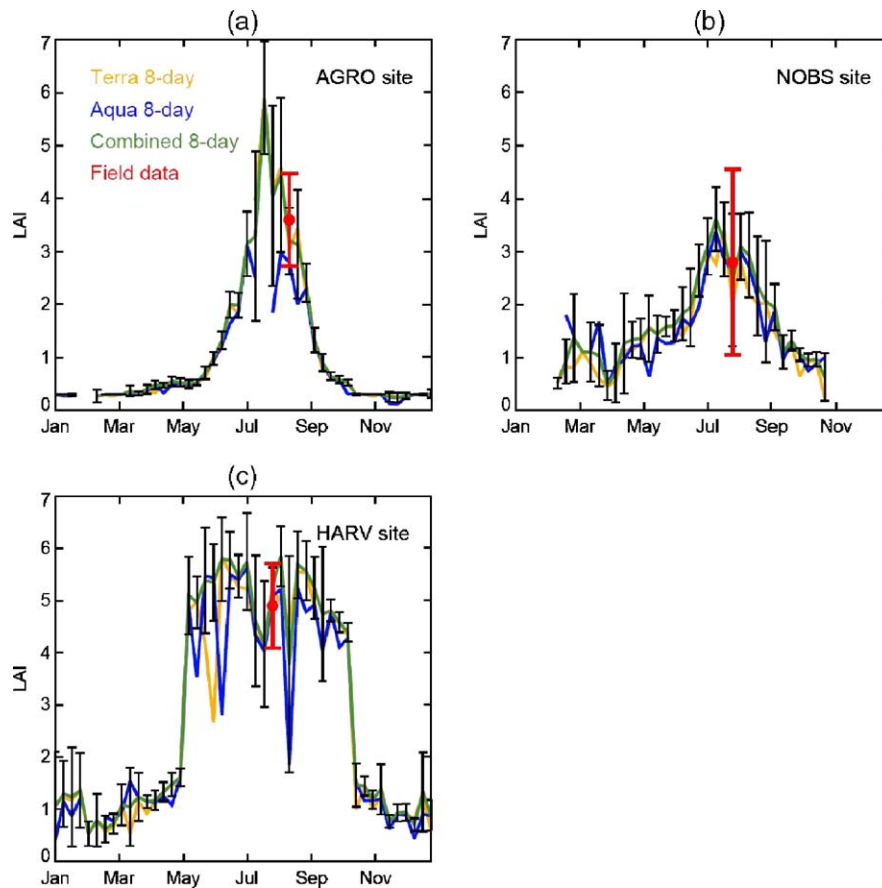
Fig. 10. Comparison of Terra MODIS 8-day, Aqua MODIS 8-day, and Terra–Aqua combined 8-day LAI retrievals with field measurements at three sites in North America. Field data were collected by Cohen et al. (2003) at the following sites—AGRO (broadleaf crops, 40.0066580°N/88.291535°E, MODIS tile h11v04, sample 284, line 1199), NOBS (needle leaf forests, 55.885260°N/98.477268°E, tile h12v03, sample 572, line 493), and HARV (broadleaf forests, 42.528513°N/72.172907°E, MODIS tile h12v04, sample 817, line 896). The annual cycle of MODIS LAI was derived from main algorithm retrievals only (with and without saturation).

validation site ($7 \times 7 = 49$ pixels). The Terra surface reflectances from the pixels at the validation site fall within the saturation retrieval domain of the main algorithm and therefore result in LAI values of about 5. The Aqua surface reflectances from the same pixels fall outside this saturation domain resulting in abnormally low LAI values. The Aqua near-infrared reflectances are darker than Terra by 25–30% and Aqua red reflectances are brighter than Terra by 15–20% for this region.

There is also a significant discrepancy in NDVI data: average Terra NDVI is 0.85, while Aqua NDVI is 0.70 (Fig. 11c). Can one attribute the above differences in channel and NDVI data to BRDF effect only, that is, variation in surface reflectances due to variations in view/illumination geometry? Earlier research based on radiative transfer theory indicates that, while channel data depends on solar zenith angle, this effect is minimized with respect to NDVI data for dense canopies (Kaufmann et al., 2000). Next, consider Fig. 11d, which shows NDVI–LAI relationship derived from the Collection 5 LUTs of the MODIS LAI/FPAR algorithm for all view/illumination geometry (0–70°) and the corresponding relationship derived from retrievals over the HARV site. The LUTs of the MODIS algorithm follow the above-mentioned radiative transfer result and show low variations in NDVI for LAI>3. The retrievals are consistent with LUTs—low Aqua NDVI results in low LAI. Note also that this anomaly cannot be attributed to cloud con-

tamination (Section 2.3). Therefore, we conclude that the retrieval anomaly over broadleaf forests should be due to limited accuracy of atmospheric correction.

The seasonality in needle leaf forest LAI retrievals was investigated further using the NOBS validation site as a test case. Two growing season composites were selected: Julian days 201–208 (July 19–26) and 249–256 (September 5–12) in year 2004. A scatter plot of Terra MODIS surface reflectances of all needle leaf forest pixels in tile h12v03 is shown in Fig. 12a–b. The July Aqua and Terra surface reflectances from the 49 pixels at the NOBS validation site are located within the retrieval domain of the main algorithm and result in LAI values of about 3, which compares well with field observations (Fig. 10b). In September, the Aqua data are compactly located while Terra data demonstrate considerable scatter. In northerly latitudes, where the NOBS site is located, the view zenith angle (VZA) is nearly constant (∼25°) and the solar zenith angle (SZA) changes from 37° in July to 54° in September. The functional dependence between red reflectance and LAI, and between near-infrared reflectance and LAI, embedded in the Look-Up-Tables of the main algorithm is shown in Fig. 12c–d for the cases which best fit the view/illumination conditions of Aqua MODIS data (VZA=30° and SZA=30°, 60°). The model simulations indicate increasing near-infrared reflectance with increasing SZA, given constant VZA.
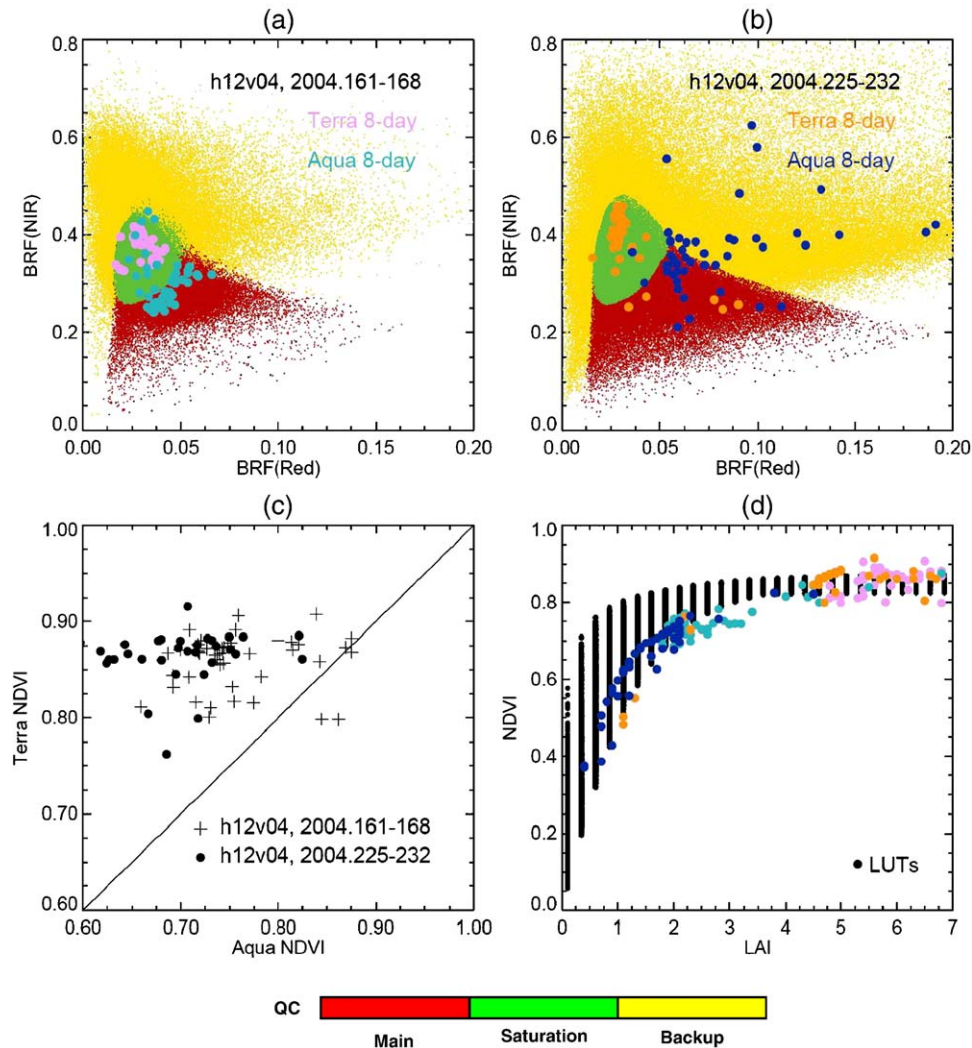
Fig. 11. Analysis of Terra and Aqua MODIS LAI retrievals from broadleaf forest pixels in tile h12v04 containing the validation site at Harvard Forest (site HARV of Cohen et al., 2003). Panel (a) shows scatter plot of Terra MODIS surface reflectances over broadleaf forests in tile h12v04 during Julian days 161–168 (June 9–16) in year 2004. The color coding corresponds to different processing branches of the MODIS LAI/FPAR algorithm. The Terra MODIS 8-day and Aqua MODIS 8-day surface reflectances from the HARV site during the same compositing period are also shown in this panel. Panel (b) shows the same but for compositing period 225–232 (August 12–19) in year 2004. Panel (c) compares Terra 8-day and Aqua 8-day NDVI for the above composing periods. Panel (d) shows LUTs of the main LAI/FPAR algorithm (LAI–NDVI relationship) overlaid with Terra and Aqua retrievals during the above compositing periods.

The Aqua MODIS data show the opposite—decreasing near-infrared reflectance with increasing SZA, at a constant VZA (Fig. 12d). This inconsistency is likely responsible for the observed seasonality in needle leaf forest LAI retrievals. While the physics behind this inconsistency is not known, at least four reasons can be put forth—(1) incomplete atmospheric correction of MODIS observations from northerly latitudes during September–March when SZA is very high, (2) the observed changes in the MODIS surface reflectances may be due to seasonality in understory, (3) change in needle optical properties, and (4) deficiency of radiative transfer model to capture the physics. This is a topic of investigation in its own right in the future.

4. Conclusions

A prototype product suite, containing the Terra 8-day, Aqua 8-day, Terra–Aqua combined 8- and 4-day products, was generated over North America as part of testing for the next version of MODIS LAI/FPAR products—the Collection 5. The following conclusions can be drawn from analyses of these products.

There are no significant discrepancies between Terra and Aqua 8-day reflectances and LAI products, averaged over large areas, ranging from continent to MODIS tile. However, there can be large differences at smaller scales, typically validation sites of the order of a few kilometers, due to the random nature of residual atmospheric effect.

In Collection 5, high quality radiative transfer based retrievals can be expected in 90–95% of the pixels with mostly herbaceous cover and about 50–75% of the pixels with woody vegetation during the growing season. The number of high quality retrievals during the growing season is mostly restricted by aerosol contamination of the MODIS data. The Terra–Aqua combined 8-day product helps to minimize this
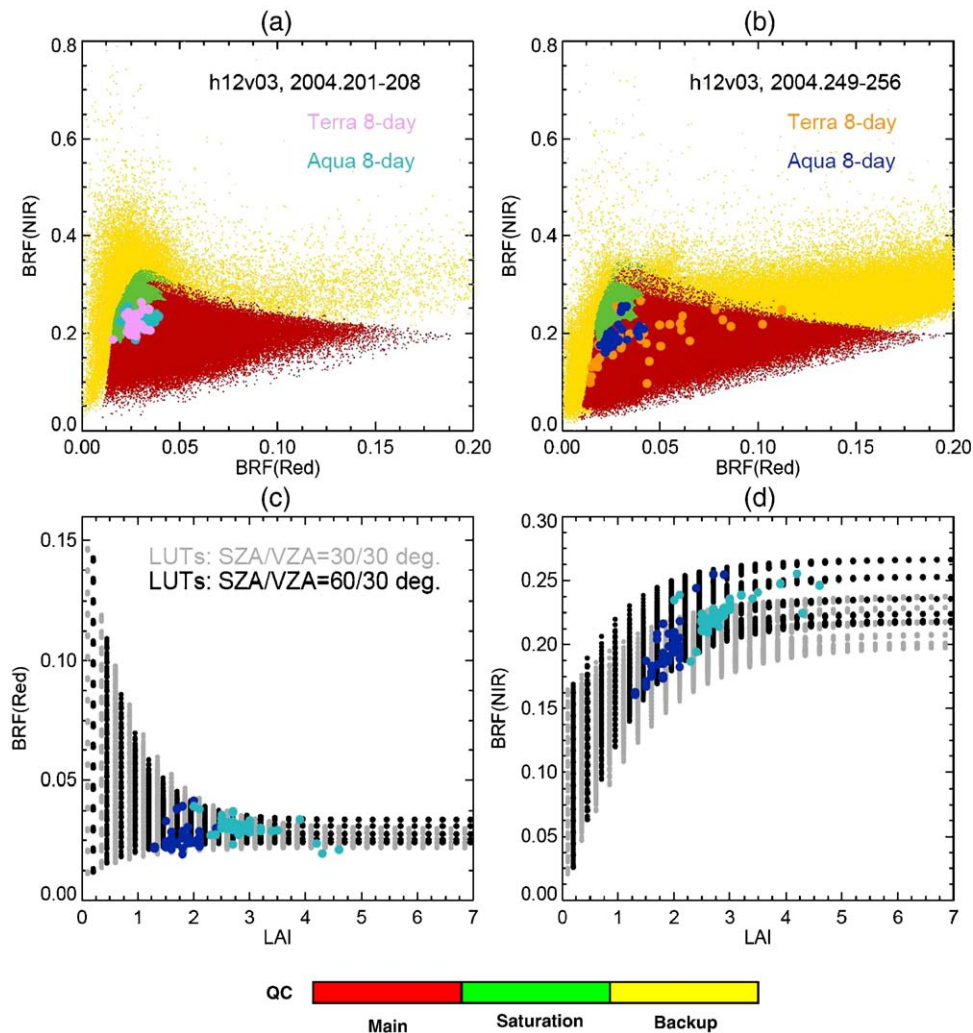
Fig. 12. Analysis of Terra and Aqua MODIS LAI retrievals from needle leaf forest pixels in tile h12v03 containing the validation site NOBS of Cohen et al. (2003). Panel (a) shows scatter plot of Terra MODIS surface reflectances over needle leaf forest pixels in tile h12v03 during Julian days 201–208 (July 19–26) in year 2004. The color coding corresponds to different processing branches of the MODIS LAI/FPAR algorithm. Also shown are Terra MODIS 8-day and Aqua MODIS 8-day surface reflectances over the NOBS site during the same compositing period. Panel (b) shows the same but for compositing period 249–256 (September 5–12) in year 2004. Panel (c) shows the LAI–BRF(red) relationship generated from the Look-Up-Table (LUT) entries of the main LAI/FPAR algorithm along with Terra and Aqua MODIS retrievals during the above two compositing periods. Panel (d) shows the same but for LAI–BRF(NIR) relationship.

effect and increases the number of high quality retrievals by 10–20% over woody vegetation. The combined product did not result in more main algorithm retrievals during the winter period because of the persistence of snow. That is, if the Terra observations are snow contaminated, the Aqua observations are also snow contaminated, as the two differ by only 3 h. This was also the case with respect to cloud contamination— the proportion of cloudy pixels in single-sensor and combined product was similar.

There are also no significant discrepancies between the single-sensor 8-day products and the combined 4-day product. The LAI magnitudes, seasonal profiles, and the proportion of higher quality retrievals are comparable amongst these products. Thus, the combined 4-day product may be used in many applications in lieu of the 8-day product to facilitate phenology monitoring during vegetation transition periods.

Both Terra and Aqua LAI products show anomalous seasonality in boreal needle leaf forests, due to limitations of the RT model to simulate seasonal variations observed in MODIS surface reflectance data with respect to solar zenith angle. This needs to be investigated further utilizing comprehensive field measurements through the seasonal cycle. Finally, this study suggests that further improvement of the MODIS LAI products is mainly restricted by the accuracy of the MODIS observations.

Acknowledgements

References

Ahl, D. E., Gower, S. T., Burrows, S. N., Shabnaov, N. V., Myneni, R. B., & Knyazikhin, Y. (2006-this issue). Monitoring spring canopy phenology of a deciduous broadleaf forest using MODIS. *Remote Sensing of Environment*. doi:10.1016/j.rse.2006.05.003

Baret, F., Morissette, J., Fernandes, R., Champeaux, J. L., Mynenei, R. B., Chen, J., et al. (2006). Evaluation of the representativeness of networks of sites for the validation and inter-comparison of global land biophysical products. Proposition of the CEOS-BELMANIP. *IEEE Transactions on Geoscience and Remote Sensing* (in print).

Bonan, G. B., Oleson, K. W., Vertenstein, M., & Levis, S. (2003). The land surface climatology of the community land model coupled to the NCAR community climate model. *Journal of Climate*, *15*, 3123–3149.

Botta, A., Viovy, N., & Ciais, P. (2000). A global prognostic scheme of leaf onset using satellite data. *Global Change Biology*, *6*, 709–725.

Chuine, I., Belmonte, J., & Mignot, A. (2000). A modeling analysis of the genetic variation of phenology between tree populations. *Journal of Ecology*, *88*, 561–570.

Cohen, W. B., Maiersperger, T. K., Yang, Z., Gower, S. T., Turner, D. P., Ritts, W. D., et al. (2003). Comparisons of land cover and LAI estimates derived from ETM+ and MODIS for four sites in North America: A quality assessment of 2000/2001 provisional MODIS products. *Remote Sensing of Environment*, *88*, 233–255.

Dickinson, R. E., Henderson-Sellers, A., Kennedy, P. J., & Wilson, M. F. (1986). *Biosphere–Atmosphere Transfer Scheme (BATS) for the NCAR CCM, NCAR/TN-275-STR*. Boulder, CO: NCAR Research.

Fensholt, R., Sandholt, I., & Rasmussen, M. S. (2004). Evaluation of MODIS LAI, fAPAR and the relation between fAPAR and NDVI in a semi-arid environment using in situ measurements. *Remote Sensing of Environment*, *91*, 490–507.

Flowers, E. C., McCormick, R. A., & Kurfis, K. R. (1969). Atmospheric turbidity over the United States, 1961–1966. *Journal of Applied Meteorology*, *8*, 955–962.

Friedl, M. A., McIver, D. K., Hodges, J. C. F., Zhang, X. Y., Muchoney, D., Strahler, A. H., et al. (2002). Global land cover mapping from MODIS: Algorithms and early results. *Remote Sensing of Environment*, *83*, 287–302.

Heinsch, F. A., Zhao, M., Running, S. W., Kimball, J. S., Nemani, R. R., Davis, K. J., et al. (2006). Evaluation of remote sensing based terrestrial productivity from MODIS using regional tower eddy flux network observations. *IEEE Transactions on Geoscience and Remote Sensing* (in press).

Holben, B. N., Tanre, D., Smirnov, A., Eck, T. F., Slutsker, I., Abuhassan, N., et al. (2001). An emerging ground-based aerosol climatology: Aerosol optical depth from AERONET. *Journal of Geophysical Research*, *106*(D11), 12067–12097.

Huang, D., Yang, W., Tan, B., Rautiainen, M., Zhang, P., Shabanov, N. V., et al. (2006). The importance of measurement error for deriving accurate reference leaf area index maps for validation of the MODIS LAI product. *IEEE Transactions on Geoscience and Remote Sensing* (in print).

Huemmrich, K. F., Privette, J. L., Mukelabai, M., Myneni, R. B., & Knyazikhin, Y. (2005). Time-series validation of MODIS land biophysical products in a Kalahari woodland, Africa. *International Journal of Remote Sensing*, *26*, 4381–4398.

Justice, C. O., Townshend, J. R. G., Vermote, E. F., Masuoka, E., Wolfe, R. E., El-Saleous, N., et al. (2002). An overview of MODIS land data processing and product status. *Remote Sensing of Environment*, *83*, 3–15.

Kang, S., Running, S. W., Lim, J. -H., Zhao, M., Park, C. -R., & Loehman, R. (2003). A regional phenology model for detecting onset of greenness in temperate mixed forests, Korea: An application of MODIS leaf area index. *Remote Sensing of Environment*, *86*, 232–242.

Kaufmann, R. K., Zhou, L., Knyazikhin, Y., Shabanov, N. V., Myneni, R. B., & Tucker, C. J. (2000). Effect of orbital drift and sensor changes on the time series of AVHRR vegetation index data. *IEEE Transactions on Geoscience and Remote Sensing*, *38*(6), 2584–2597.

King, M. D., Kaufman, Y. J., Menzel, W. P., & Tanre, D. (1992). Remote sensing of cloud, aerosol, and water vapor properties from the Moderate Resolution Imaging Spectrometer (MODIS). *IEEE Transactions on Geoscience and Remote Sensing*, *30*(1), 2–27.

Knyazikhin, Y., Martonchik, J. V., Myneni, R. B., Diner, D. J., & Runing, S. (1998). Synergistic algorithm for estimating vegetation canopy leaf area index and fraction of absorbed photosynthetically active radiation from MODIS and MISR data. *Journal of Geophysical Research*, *103*, 32257–32275.

Kobayashi, H., & Dye, D. G. (2005). Atmospheric conditions for monitoring the long-term vegetation dynamics in the Amazon using normalized difference vegetation index. *Remote Sensing of Environment*, *97*(4), 519–525.

Morisette, J. T., Baret, F., Privette, J. L., Myneni, R. B., Nickeson, J., Garrigues, S., et al. (2006). Validation of global moderate resolution LAI products: A framework proposed within the CEOS land product validation subgroup. *IEEE Transactions on Geoscience and Remote Sensing* (in print).

Morisette, J. T., Privette, J. L., & Justice, C. O. (2002). A framework for the validation of MODIS land products. *Remote Sensing of Environment*, *83*, 77–96.

Myneni, R. B., Hoffman, S., Knyazikhin, Y., Privette, J. L., Glassy, J., Tian, Y., et al. (2002). Global products of vegetation leaf area and fraction absorbed PAR from year one of MODIS data. *Remote Sensing of Environment*, *83*, 214–231.

Myneni, R. B., Keeling, C. D., Tucker, C. J., Asrar, G., & Nemani, R. R. (1997). Increased plant growth in the northern high latitudes from 1981 to 1991. *Nature*, *386*, 698–702.

Peterson, J. T., Flowers, E. C., Berri, G. J., Reynolds, C. L., & Rudisill, J. H. (1981). Atmospheric turbidity over central North Carolina. *Journal of Applied Meteorology*, *20*, 229–242.

Potter, C., Kloster, S., Genovese, V., & Myneni, R. B. (2003). Satellite data help predict terrestrial carbon sinks. *EOS*, *84*(46), 502–508.

Privette, J. L., Myneni, R. B., Knyazikhin, Y., Mukufute, M., Roberts, G., Tian, Y., et al. (2002). Early spatial and temporal validation of MODIS LAI product in Africa. *Remote Sensing of Environment*, *83*, 232–243.

Ramanathan, V., Crutzen, P. J., Kiehl, J. T., & Rosenfeld, D. (2001). Aerosols, climate, and the hydrological cycle. *Science*, *294*, 2119–2124.

Salomonson, V. V., Barnes, W. L., Maymon, P. W., Montgomery, H. E., & Ostrow, H. (1989). MODIS: Advanced facility instrument for studies of the earth as a system. *IEEE Transactions on Geoscience and Remote Sensing*, *27*(2), 145–153.

Shabanov, N. V., Huang, D., Yang, W., Tan, B., Knyazikhin, Y., Myneni, R. B., et al. (2005). Analysis and optimization of the MODIS leaf area index algorithm retrievals over broadleaf forests. *IEEE Transactions on Geoscience and Remote Sensing*, *43*(8), 1855–1865.

Shabanov, N. V., Knyazikhin, Y., Baret, F., & Myneni, R. B. (2000). Stochastic modeling of radiation regime in discontinuous vegetation canopies. *Remote Sensing of Environment*, *74*(1), 125–144.

Sparks, T. H., & Menzel, A. (2002). Observed changes in season: An overview. *International Journal of Climatology*, *22*, 1715–1725.

Tan, B., Hu, J., Zhang, P., Huang, D., Shabanov, N. V., Weiss, M., et al. (2005). Validation of moderate resolution imaging spectroradiometer leaf area index product in croplands of Alpilles, France. *Journal of Geophysical Research, Atmosphere*, *110*(D01), 107. doi:10.1029/2004JD004860

Tan, B., Hu, J., Huang, D., Yang, W., Zhang, P., Shabanov, N. V., et al. (2005). Assessment of the broadleaf crops leaf area index product from the Terra MODIS instrument. *Agricultural and Forest Meteorology*, *135*, 124–134.

Tian, Y., Dickinson, R. E., Zhou, L., Zeng, X., Dai, Y., Myneni, R. B., et al. (2004). Comparison of seasonal and spatial variations of leaf area index and fraction of absorbed photosynthetically active radiation from Moderate Resolution Imaging Spectroradiometer (MODIS) and Common Land Model. *Journal of Geophysical Research, Atmosphere*, *109*(D01), 103. doi:10.1029/2003JD003777

Schwartz, M. (1998). Green-wave phenology. *Nature*, *394*, 839–840.

Vermote, E. F., El-Saleous, N., & Justice, C. O. (2002). Atmospheric correction of MODIS data in visible to middle infrared: first results. *Remote Sensing of Environment*, *83*, 97–111.

Vermote, E. F., El-Saleous, N., Justice, C. O., Kaufman, Y. J., Privette, J. L., Remer, L., et al. (1997). Atmospheric correction of visible to middle-infrared EOS-MODIS data over land surfaces: Background, operational algorithm and validation. *Journal of Geophysical Research, Atmosphere*, *102*(D14), 17131–17141.

Wang, Y., Woodcock, C. E., Buermann, W., Stenberg, P., Voipio, P., Smolander, H., et al. (2002). Evaluation of the MODIS LAI algorithm at a coniferous forest site in Finland. *Remote Sensing of Environment, 91*, 114–127.

White, M. A., Thornton, P. E., & Running, S. W. (1997). *A continental phenology model for monitoring vegetation responses to interannual climatic variability.*

WWW1: Land Processes Distributed Active Archive Center, http://lpdaac.usgs.gov/main.asp

WWW2: MODIS tiles, http://modland.nascom.nasa.gov/developers/grids.html

WWW3: Global browse of MODIS Land products, http://landqa2.nascom.nasa.gov/cgi-bin/browse/browse.cgi

WWW4: MODIS ASCII subsets over FLUXNET sites, http://daacsti.ornl.gov/cgi-bin/MODIS/GR_1/button.slim.pl

WWW5: AERONET sunphotometers network, http://aeronet.gsfc.nasa.gov/

Yang, W., Tan, B., Huang, D., Rautiainen, M., Shabanov, N. V., Wang, Y., et al. (2006a). MODIS leaf area index products: From validation to algorithm improvement. *IEEE Transactions on Geoscience and Remote Sensing* (in print).

Yang, W., Huang, D., Tan, B., Stroeve, J. C., Shabanov, N. V., Knyazikhin, Y., et al. (2006b). Analysis of leaf area index and fraction of PAR absorbed by vegetation products from the Terra MODIS sensor: 2000–2005. *IEEE Transactions on Geoscience and Remote Sensing* (in print).

Zhang, X., Friedl, M. A., Schaaf, C. B., & Strahler, A. H. (2005). Monitoring the response of vegetation phenology to precipitation in Africa by coupling MODIS and TRMM instruments. *Journal of Geophysical Research, 110* (D12103). doi:10.1029/2004JD005263